PROCEEDINGS OF SCIENCE

Two-loop helicity amplitudes for W/Z boson pair production in gluon fusion with exact top mass dependence

Christian Brønnum-Hansen* **and Chen-Yu Wang**

Institute for Theoretical Particle Physics, KIT, Karlsruhe, Germany

E-mail: christian.broennum-hansen@kit.edu, chen-yu.wang@kit.edu

We compute the top quark contribution to the two-loop amplitudes for on-shell W/Z boson pair production in gluon fusion, $gg \to WW$ and $gg \to ZZ$. Exact dependence on the top quark mass is retained, the bottom quark is considered massless. Integral reduction is performed numerically for each phase space point and the master integrals are evaluated using the auxiliary mass flow method. This allows for fast computation of the amplitudes to very high precision.

Loops and Legs in Quantum Field Theory - LL2022,
25-30 April, 2022
Ettal, Germany

*Speaker

https://pos.sissa.it/

PoS(LL2022)030

1. Introduction

Vector boson pair production $pp \to VV$ is an important process at the LHC. It is part of the irreducible background to the Higgs boson decay $H \to 4l/2l2\nu$. Precise determination of the Higgs decay cross section in the off-shell region provides a constraint on the Higgs width [1–5]. Vector boson pair production contributes a sizeable correction through interference effects with the off-shell Higgs decay. Furthermore, this process can be used to test the Standard Model by probing anomalous gauge couplings. Therefore a reliable description of this production mode is essential.

The gluon fusion channel $gg \to VV$ is loop-induced and formally enters $pp \to VV$ at next-to-next-to-leading order (NNLO) QCD. Despite being suppressed by the strong coupling constant, the large gluon flux at the LHC as well as event selection enhance the contribution of the gluon fusion channel to the hadronic cross section [6]. The leading order (LO) contribution has been known for a long time [6–9], the next-to-leading order (NLO) real correction is also available in the literature [10–12]. Several years ago, the NLO virtual correction with massless internal quarks was calculated and found to be quite large [13, 14]. The two-loop correction can reach 50% at partonic level, which in turn yields a contribution to the hadronic cross section of 6 - 8% for $\sigma_{pp\to ZZ}$ and 2% for $\sigma_{pp\to WW}$. A previous study shows that the massive third generation increases $\sigma_{gg\to WW}$ by 10% at LO, and dominates in the high p_t region [15]. This motivates inclusion of the top quark contribution to the NLO virtual correction. Multiple works have been devoted to calculating massive quark contributions [16–18], where approximations were applied to simplify the problem. Recently, full top quark mass effects were computed numerically for both WW [19] and ZZ [20, 21] production by two independent groups. In these proceedings, we present our calculation method: we perform integration-by-part reductions for each phase space point and evaluate master integrals using the auxiliary mass flow method [22–24]. This paper is organised as follows. In Section 2 we describe the amplitude calculation and discuss the numerical methods applied in the integral reduction and master integral evaluation. We present our results in Section 3.

2. Calculational setup

We consider the process

$$g(p_1) + g(p_2) \to V(p_3) + V(p_4), \tag{1}$$

where $V = W$ or Z. This process is loop-induced and proceeds through a fermion loop. Our goal is to calculate the scattering amplitude for these processes at two-loop order in QCD with fermion loops involving massive top quarks.[1] Representative Feynman diagrams for the two different final states are given in Table 1. We do not consider diagrams with intermediate Z- or Higgs bosons as these are already available in the literature [6, 25–28].

The scattering amplitudes can be decomposed in colour factors

$$A = \delta^{AB}\left(C_A A^{[C_A]} + C_F A^{[C_F]} + A^{[\triangle^2]}\right), \tag{2}$$

[1] We refer the reader to Refs. [19, 20] for detailed descriptions of our calculations.

$gg \to WW$	$gg \to ZZ$

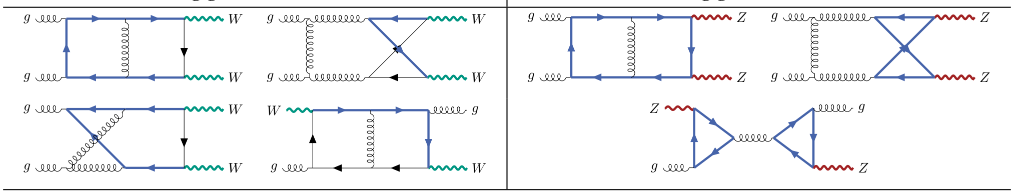

Table 1: Representative diagrams for the two final states considered. Blue fermion lines represent the top quarks. For WW there is a total of 136 diagrams while there are 138 for ZZ.

where $C_A = N_C$ and $C_F = \frac{N_C^2-1}{2N_C}$ are the Casimir elements of $SU(N_C)$ where $N_C = 3$ is the number of colours. A and B are the adjoint colour indices of the gluons. All factorisable diagrams are contained in $A^{[\triangle^2]}$ which vanishes for the final state $V = W$. In these proceedings we do not consider the factorisable contribution, indeed we keep only contributions proportional to C_A or C_F.

We work in dimensional regularisation and set $d = 4 - 2\epsilon$. The electroweak vertices have an axial contribution and therefore introduce the γ_5 matrix. As γ_5 is defined in four dimensions, a prescription for dealing with this matrix in dimensional regularisation is required. For $V = Z$ we can use a naive scheme, in which we retain the anti-commutative property of γ_5 in d dimensions, for all diagrams except those contributing to $A^{[\triangle^1]}$. For these diagrams as well as all diagrams for $V = W$ we employ the Larin scheme [29, 30].

We project the amplitudes onto 36 tensor structures, T_I and S_I,

$$A = \sum_{I=1}^{18} A_I \underbrace{T_I}_{\text{parity even}} + \sum_{I=19}^{36} A_I \underbrace{S_I}_{\text{parity odd}} . \tag{3}$$

As the scattering amplitude for $V = Z$ is parity even, the second sum is only relevant for $V = W$. Expressions for the tensor structures is given in Ref. [6]. The form factors, A_I, contain scalar Feynman integrals that can be reduced to a set of master integrals (MIs) through integration-by-parts (IBP) reduction.

We perform the reductions with KIRA 2.2 [31, 32] for individual phase space points keeping only the dimension, d, as a parameter. The masses are set to integer values

$$m_t = 173 \text{ GeV}, \quad m_W = 80 \text{ GeV}, \quad m_Z = 91 \text{ GeV}, \tag{4}$$

and for the kinematic invariants $s = (p_1 + p_2)^2$ and $t = (p_1 - p_3)^2$ we use rational values.[2] A summary of the complexity and computational expense is given in Table 2. The reductions are performed on single cores and the relatively low memory consumption allows for straightforward parallelisation.

Having expressed the form factors, A_I, in terms of master integrals, the final step of the calculation is to evaluate these integrals. We evaluate the master integrals numerically using a method based on auxiliary mass flow [22–24]. Details on our implementation are given in Refs. [19, 20]. Here, we briefly summarise the procedure. At variance with the original formulation

[2] This is different to the calculation in Ref. [19] where the reduction was parametric in s and t.

PoS(LL2022)030

	$gg \to WW$	$gg \to ZZ$
IBP families	33	21
highest rank	5	4
MI families	22	15
MIs	334	205
CPU h / point	8	3
Memory GB	5	2

Table 2: Summary of IBP reduction including computational expense for the two final states considered. The number of families and master integrals (MIs) is higher for the WW final state due to more possibilities for the internal flavour flow.

$gg \to WW$ | $gg \to ZZ$

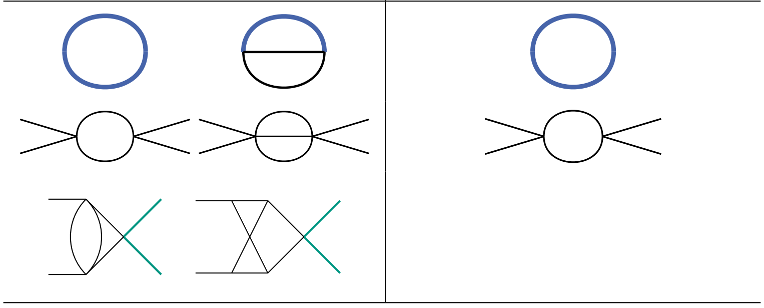

Table 3: Integrals required to compute the boundary conditions for all master integrals. Solid blue lines are massive, black lines are massless. Analytic expressions for all boundary integrals can be found in the literature.

of this method, we add the auxiliary mass, η, to the massive propagators only, i.e. $m_t \to m_t - i\eta$. We then construct analytic differential equations with respect to η and obtain boundary conditions in the limit $\eta \to \infty$. In this limit, all the master integrals can be expressed in terms of a handful of simpler integrals. The necessary integral topologies are depicted in Table 3 and analytic expressions for the integrals can be found in the literature [33–37].

We proceed by inserting generalised power series expansions for the master integrals, $\boldsymbol{I}$, in the differential equation,

$$\boldsymbol{I} = \sum_j \epsilon^j \sum_k \sum_l \boldsymbol{c}_{jkl} \left(\frac{1}{\eta}\right)^k \ln^l(\eta) + \ldots, \tag{5}$$

and solve the resulting system numerically for the coefficients $\boldsymbol{c}_{jkl}$ and impose the boundary condition. The radius of convergence of such expansions are limited by the distance to the nearest singularity of the differential equation. By evaluating at a point within this radius and performing a new expansion around this point, we can step by step transport the master integrals back to the physical mass at $\eta = 0$. Note that at all intermediate, as well as at he final point $\eta = 0$, the differential equation admits simple Taylor expansions in η for the integrals.

A very important observation is that this procedure provides full control of the numerical precision. The precision can always be improved by increasing the order of expansion in the power series and by taking smaller steps within the radius of convergence of the expansions. In our case, we obtain results with around 15 digits of precision for $V = W$ and 20 digits for $V = Z$ in one hour on a single core. The memory consumption is negligible and the evaluation of master integrals is therefore easy to parallelise. With efficient and precise evaluation of the master integrals, we can present results for scans of phase space at modest computational expense.

3. Results

To present our results, we parametrise the phase space in terms of the relative velocity β and scattering angle θ,

$$s = (p_1 + p_2)^2 = \frac{4m_V^2}{1-\beta^2}, \qquad t = (p_1 - p_3)^2 = m_V^2 - \frac{s}{2}(1 - \beta\cos\theta)\ . \tag{6}$$

The procedure to evaluate the form factors, A_I, is described above. The tensor structures, T_I and S_I are evaluated by constructing polarisation vectors for the external particles using spinor-helicity formalism. For the gluons the polarisation vectors are given by

$$\epsilon^{\mu}_{1,L} = -\frac{1}{\sqrt{2}}\frac{[2|\gamma^\mu|1\rangle}{[21]}, \quad \epsilon^{\mu}_{1,R} = \frac{1}{\sqrt{2}}\frac{\langle 2|\gamma^\mu|1]}{\langle 21\rangle}, \tag{7}$$

$$\epsilon^{\mu}_{2,L} = -\frac{1}{\sqrt{2}}\frac{[1|\gamma^\mu|2\rangle}{[12]}, \quad \epsilon^{\mu}_{2,R} = \frac{1}{\sqrt{2}}\frac{\langle 1|\gamma^\mu|2]}{\langle 12\rangle}\ . \tag{8}$$

We write the massive boson polarisation vectors in terms of decay currents

$$\epsilon^{*\mu}_{3,L} = \langle 5|\gamma^\mu|6], \qquad \epsilon^{*\mu}_{4,L} = \langle 7|\gamma^\mu|8], \tag{9}$$

where we decompose the massive momenta into four massless momenta vectors for $p_3 = p_5 + p_6$ and $p_4 = p_7 + p_8$. For both final states there are two independent helicity configurations.

The renormalised, two-loop scattering amplitudes[3] have a universal infrared pole structure [38] given by

$$A^{(2)}(\epsilon,\mu) = I^{(1)}(\epsilon,\mu)A^{(1)}(\epsilon,\mu) + F^{(2)}(\epsilon,\mu), \tag{10}$$

where

$$I^{(1)}(\epsilon,\mu) = -\frac{e^{\epsilon\gamma_E}}{\Gamma(1-\epsilon)}\left(\frac{C_A}{\epsilon^2} + \frac{\frac{11}{6}C_A}{\epsilon}\right)\left(\frac{\mu^2 e^{i\pi}}{s}\right)^{\epsilon}, \tag{11}$$

and $F^{(2)}(\epsilon,\mu)$ is a finite remainder. The superscripts on A and F denote loop order and we expand $A^{(1)}(\epsilon,\mu)$ to $O(\epsilon^2)$. In Tables 4 and 5 we compare the infrared pole structure prediction to our evaluation of the amplitudes for WW and ZZ respectively. We find agreement to at least 10 digits on the ϵ^{-2} pole.

We proceed by scanning the phase space and calculate the quantity

$$\frac{2\,\mathrm{Re}\left[F^{(2)}(\epsilon,\mu)A^{(1)\star}(\epsilon,\mu)\right]}{|A^{(1)}(\epsilon,\mu)|^2}, \tag{12}$$

[3]See Refs. [19, 20] for details on our renormalisation procedure.

$\mathbf{C_A}$		ϵ^{-2}	ϵ^{-1}
LLLL	$A^{(2)}/A^{(1)}$	$1.00000000023 - 3.0 \cdot 10^{-11} i$	$-4.94945452453 + 3.89380807761 i$
	IR pole	1.00000000000	$-4.94945452593 + 3.89380807754 i$
LRLL	$A^{(2)}/A^{(1)}$	$0.99999999815 - 1.6 \cdot 10^{-9} i$	$-4.29712348534 + 9.47440879823 i$
	IR pole	1.00000000000	$-4.29712347965 + 9.47440880940 i$

Table 4: Comparison of the renormalised two-loop amplitude for $gg \to WW$, normalised to the finite one-loop amplitude, and the infrared (IR) pole prediction at a phase space point given by Eq. (6) with $\sqrt{s} \approx 367$ GeV and $\theta \approx 36.9°$, with $\mu = m_W$.

$\mathbf{C_A}$		ϵ^{-2}	ϵ^{-1}
LLLL	$A^{(2)}/A^{(1)}$	$1.0000000000008 - 7.6 \cdot 10^{-13} i$	$0.8304916142577 + 3.229874368770 i$
	IR pole	1.0000000000000	$0.8304916142539 + 3.229874368771 i$
LRLL	$A^{(2)}/A^{(1)}$	$1.0000000000009 - 1.4 \cdot 10^{-12} i$	$0.2359507533599 + 2.885154863850 i$
	IR pole	1.0000000000000	$0.2359507533772 + 2.885154863852 i$

Table 5: Comparison of the renormalised two-loop amplitude for $gg \to ZZ$, normalised to the finite one-loop amplitude, and the infrared (IR) pole prediction at a phase space point given by Eq. (6) with $\sqrt{s} \approx 210$ GeV and $\theta \approx 114°$, with $\mu = m_Z$.

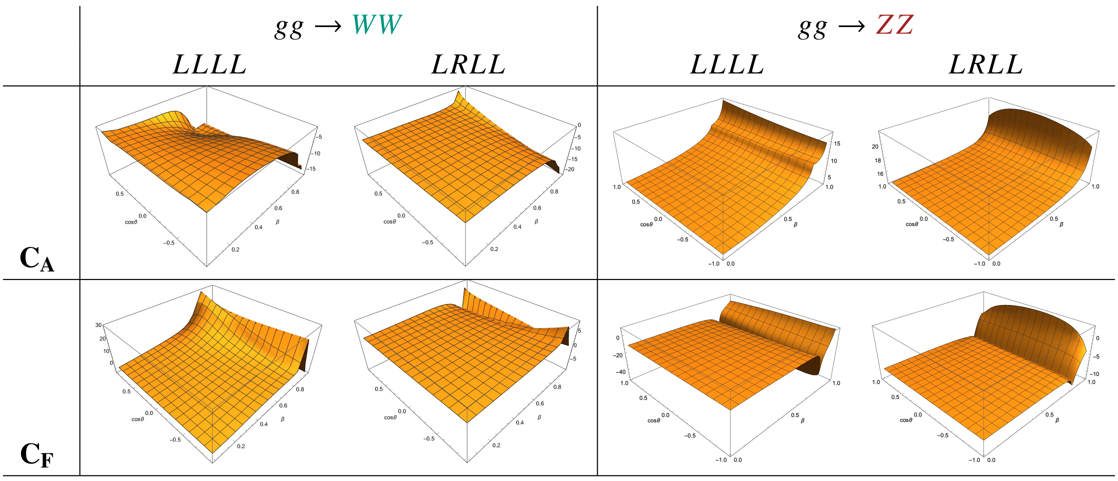

Table 6: Plots of normalised, two-loop remainders defined in Eq. (12) for the two processes for the two independent helicity configurations and colour factors. The kinematic variables are defined in Eq. (6) and $\mu = m_V$ where $V = W, Z$ respectively.

as a function of β and $\cos\theta$ as defined in Eq. (6). The plots are given in Table 6. Finally, for $V = Z$ we have cross-checked our final remainders against the results of Ref. [21], which employs analytic IBP reduction and sector decomposition, as well as the results of Ref. [18] which uses expansion by regions for both low- and high energy.

Acknowledgments

We would like to thank the organisers of Loops and Legs 2022 for the opportunity to present this work. This research is partially supported by the Deutsche Forschungsgemeinschaft (DFG, German Research Foundation) under grant 396021762 - TRR 257.

References

[1] J.M. Campbell, R. Ellis and C. Williams, *Gluon-Gluon Contributions to W+ W- Production and Higgs Interference Effects*, *JHEP* **10** (2011) 005 [1107.5569].

[2] N. Kauer and G. Passarino, *Inadequacy of zero-width approximation for a light Higgs boson signal*, *JHEP* **08** (2012) 116 [1206.4803].

[3] F. Caola and K. Melnikov, *Constraining the Higgs boson width with ZZ production at the LHC*, *Phys. Rev. D* **88** (2013) 054024 [1307.4935].

[4] J.M. Campbell, R.K. Ellis and C. Williams, *Bounding the Higgs Width at the LHC: Complementary Results from $H \to WW$*, *Phys. Rev. D* **89** (2014) 053011 [1312.1628].

[5] A. Azatov, C. Grojean, A. Paul and E. Salvioni, *Taming the off-shell Higgs boson*, *Zh. Eksp. Teor. Fiz.* **147** (2015) 410 [1406.6338].

[6] T. Binoth, M. Ciccolini, N. Kauer and M. Kramer, *Gluon-induced W-boson pair production at the LHC*, *JHEP* **12** (2006) 046 [hep-ph/0611170].

[7] E. Glover and J. van der Bij, *VECTOR BOSON PAIR PRODUCTION VIA GLUON FUSION*, *Phys. Lett. B* **219** (1989) 488.

[8] C. Kao and D.A. Dicus, *Production of W+ W- from gluon fusion*, *Phys. Rev. D* **43** (1991) 1555.

[9] M. Duhrssen, K. Jakobs, J. van der Bij and P. Marquard, *The Process gg —> WW as a background to the Higgs signal at the LHC*, *JHEP* **05** (2005) 064 [hep-ph/0504006].

[10] P. Agrawal and A. Shivaji, *Di-Vector Boson + Jet Production via Gluon Fusion at Hadron Colliders*, *Phys. Rev. D* **86** (2012) 073013 [1207.2927].

[11] T. Melia, K. Melnikov, R. Rontsch, M. Schulze and G. Zanderighi, *Gluon fusion contribution to W+W- + jet production*, *JHEP* **08** (2012) 115 [1205.6987].

[12] F. Campanario, Q. Li, M. Rauch and M. Spira, *ZZ+jet production via gluon fusion at the LHC*, *JHEP* **06** (2013) 069 [1211.5429].

[13] F. Caola, J.M. Henn, K. Melnikov, A.V. Smirnov and V.A. Smirnov, *Two-loop helicity amplitudes for the production of two off-shell electroweak bosons in gluon fusion*, *JHEP* **06** (2015) 129 [1503.08759].

[14] F. Caola, K. Melnikov, R. Röntsch and L. Tancredi, *QCD corrections to ZZ production in gluon fusion at the LHC*, *Phys. Rev. D* **92** (2015) 094028 [1509.06734].

[15] J.M. Campbell, R. Ellis and C. Williams, *Vector boson pair production at the LHC*, *JHEP* **07** (2011) 018 [1105.0020].

[16] K. Melnikov and M. Dowling, *Production of two Z-bosons in gluon fusion in the heavy top quark approximation*, *Phys. Lett. B* **744** (2015) 43 [1503.01274].

[17] R. Gröber, A. Maier and T. Rauh, *Top quark mass effects in $gg \to ZZ$ at two loops and off-shell Higgs boson interference*, *Phys. Rev. D* **100** (2019) 114013 [1908.04061].

[18] J. Davies, G. Mishima, M. Steinhauser and D. Wellmann, *$gg \to ZZ$: analytic two-loop results for the low- and high-energy regions*, *JHEP* **04** (2020) 024 [2002.05558].

[19] C. Brønnum-Hansen and C.-Y. Wang, *Contribution of third generation quarks to two-loop helicity amplitudes for W boson pair production in gluon fusion*, *JHEP* **01** (2021) 170 [2009.03742].

[20] C. Brønnum-Hansen and C.-Y. Wang, *Top quark contribution to two-loop helicity amplitudes for Z boson pair production in gluon fusion*, *JHEP* **05** (2021) 244 [2101.12095].

[21] B. Agarwal, S.P. Jones and A. von Manteuffel, *Two-loop helicity amplitudes for $gg \to ZZ$ with full top-quark mass effects*, 2011.15113.

[22] X. Liu, Y.-Q. Ma and C.-Y. Wang, *A Systematic and Efficient Method to Compute Multi-loop Master Integrals*, *Phys. Lett. B* **779** (2018) 353 [1711.09572].

[23] X. Liu, Y.-Q. Ma, W. Tao and P. Zhang, *Calculation of Feynman loop integration and phase-space integration via auxiliary mass flow*, 2009.07987.

[24] X. Liu and Y.-Q. Ma, *Multiloop corrections for collider processes using auxiliary mass flow*, *Phys. Rev. D* **105** (2022) L051503 [2107.01864].

[25] M. Spira, A. Djouadi, D. Graudenz and P.M. Zerwas, *Higgs boson production at the LHC*, *Nucl. Phys. B* **453** (1995) 17 [hep-ph/9504378].

[26] R. Harlander and P. Kant, *Higgs production and decay: Analytic results at next-to-leading order QCD*, *JHEP* **12** (2005) 015 [hep-ph/0509189].

[27] C. Anastasiou, S. Beerli, S. Bucherer, A. Daleo and Z. Kunszt, *Two-loop amplitudes and master integrals for the production of a Higgs boson via a massive quark and a scalar-quark loop*, *JHEP* **01** (2007) 082 [hep-ph/0611236].

[28] U. Aglietti, R. Bonciani, G. Degrassi and A. Vicini, *Analytic Results for Virtual QCD Corrections to Higgs Production and Decay*, *JHEP* **01** (2007) 021 [hep-ph/0611266].

[29] S. Larin and J. Vermaseren, *The alpha-s**3 corrections to the Bjorken sum rule for polarized electroproduction and to the Gross-Llewellyn Smith sum rule*, *Phys. Lett. B* **259** (1991) 345.

[30] S. Moch, J. Vermaseren and A. Vogt, *On $\gamma 5$ in higher-order QCD calculations and the NNLO evolution of the polarized valence distribution*, *Phys. Lett. B* **748** (2015) 432 [1506.04517].

[31] J. Klappert, F. Lange, P. Maierhöfer and J. Usovitsch, *Integral Reduction with Kira 2.0 and Finite Field Methods*, 2008.06494.

[32] F. Lange, P. Maierhöfer and J. Usovitsch, *Developments since Kira 2.0*, 2111.01045.

PoS(LL2022)030

[33] G. 't Hooft and M.J.G. Veltman, *Scalar One Loop Integrals*, *Nucl. Phys. B* **153** (1979) 365.

[34] K.G. Chetyrkin, A.L. Kataev and F.V. Tkachov, *New Approach to Evaluation of Multiloop Feynman Integrals: The Gegenbauer Polynomial x Space Technique*, *Nucl. Phys. B* **174** (1980) 345.

[35] R. Scharf and J.B. Tausk, *Scalar two loop integrals for gauge boson selfenergy diagrams with a massless fermion loop*, *Nucl. Phys. B* **412** (1994) 523.

[36] T. Gehrmann and E. Remiddi, *Differential equations for two loop four point functions*, *Nucl. Phys. B* **580** (2000) 485 [hep-ph/9912329].

[37] T. Gehrmann, T. Huber and D. Maitre, *Two-loop quark and gluon form-factors in dimensional regularisation*, *Phys. Lett. B* **622** (2005) 295 [hep-ph/0507061].

[38] S. Catani, *The Singular behavior of QCD amplitudes at two loop order*, *Phys. Lett. B* **427** (1998) 161 [hep-ph/9802439].